

A Modification of the Monte Carlo Method for Simulation of Radiative Transfer in Molecular Clouds

M.A. Voronkov^{1,2}

¹ *Moscow State University, Moscow, 119899 Russia*

² *Astrospace Center, Lebedev Physical Institute, Russian Academy of Sciences,
ul. Profsovnaya 84/32, Moscow, 117810 Russia*

Received August 24, 1998

Abstract—We propose a method of simulation that is based on the averaging of formal solutions of the transfer equation by taking the integral by the Monte Carlo method. This method is used to compute two models, which correspond to the limiting cases of hot gas and cold background radiation and of hot background radiation and cold gas, for E-methanol emission from a compact homogeneous spherical region. We analyse model level populations by using rotational diagrams in the limiting cases mentioned above. Model optical depths of the lines with frequencies below 300 GHz up to $J=11$ inclusive are given.

INTRODUCTION

Molecular methanol (CH_3OH) emission, along with emission of other molecules, is commonly observed toward star-forming regions. Some molecular methanol transitions produce narrow and intense maser lines in some sources, while, in other sources, these transitions produce less intense or no detectable lines; at the same time, maser activity may show up in other transitions. The conditions for the formation of methanol masers can be studied by numerically simulating radiative transfer. In such problems, we simultaneously solve the transfer equation and the system of statistical-equilibrium equations for a large number of lines. This problem is commonly solved either by the Monte Carlo (MC) method or by large velocity gradient (LVG) method. In contrast to the LVG method, the MC method allows computations to be performed for a compact cloud and a small velocity gradient. In addition, the model adopted in the MC method admits several important complications: inhomogeneity and complex structure of an emitting cloud and a more realistic allowance for the effect of its nonspherical geometry (with no use of factor ε^{-1}). However, the MC method requires more computing time than the LVG method does. The MC method, whose algorithm was described by Bernes (1979), is based on the replacement of the real radiation field by a number of model photons and on the simulation of their propagation through the medium with the computation of the number of molecular excitations in each of the shells into which the cloud is divided. The classical MC method assumes that model photons are emitted uniformly in

all directions in each of the shells and come from the outside. Juvela (1997) proposed a modification of the standard MC method: the paths of all model photons begin at the cloud edge. However, as in the classical MC method, the formalism of model photons is used as the basis for the computations. In this paper, we make an attempt to deduce the method from the transfer equation while keeping the main features of the MC method and propose a method that is based on the averaging of formal solutions to the transfer equation by taking the integral by the Monte Carlo method. This method was tested on simulations of E-methanol emission from a compact (~ 0.005 pc) spherical cloud with no velocity gradient.

THE ALGORITHM AND BASIC APPROXIMATIONS

We performed simulations in the simplest case of a static spherical cloud with a uniform distribution of the H_2 and CH_3OH number densities and kinetic temperature. The influence of dust was ignored. The spectrum of the background radiation was assumed to follow the Plank law. The dilution of the background radiation was disregarded. The radius of the cloud was set equal to 1.5×10^{16} cm.

In the algorithm under consideration, as in the algorithm of Bernes (1979), the solution of the problem reduces to an iterative procedure which is implemented using the system of statistical-equilibrium equations (1) and which yields new approximations for the populations

$$\begin{cases} \sum_k n_k \{B_{kj}\bar{I} + A_{kj}\delta_{kj} + C_{kj}\} \\ = n_j \sum_k \{A_{jk}\delta_{jk} + B_{jk}\bar{I} + C_{jk}\} \\ \sum_k n_k = const, \end{cases} \quad (1)$$

where $\delta_{kj} = 1$ when and only when the relation between the energy levels $E_k > E_j$ holds; otherwise, $\delta_{kj} = 0$; A_{jk} and B_{jk} are the Einstein coefficients (which are assumed to be zero for forbidden transitions); C_{jk} are the collisional constants; n_k is the population of the k th level; and \bar{I} is the average intensity. In the first equation in (1), the subscript j changes in the range $1 < j < (N-1)$, where N is the total number of levels involved. The average intensity is given by

$$\bar{I} = \frac{1}{2} \int_0^{+\infty} f(\nu) d\nu \int_{-1}^{+1} I(\nu, \mu) d\mu, \quad (2)$$

where ν is the frequency, μ is the cosine of the angle between the radius and the selected direction, and $f(\nu)$ is the line profile (here it was assumed to be the Doppler profile). This integral can be calculated by the Monte Carlo method by simulating the random variables ν and μ with Gaussian (for the Doppler line profile) and uniform distributions, respectively:

$$\frac{\nu}{\nu_0} - 1 = \frac{1}{c} \left(\sigma \sin(2\pi R) (-\ln R')^{1/2} + v(r)\mu \right) \quad (3)$$

$$\mu = 1 - 2R'', \quad (4)$$

where R , R' and R'' are independent random variables with a uniform distribution in the interval 0 to 1; ν_0 is the rest frequency of the transition under consideration; $v(r)$ is the velocity field at a given point; and σ is the Doppler halfwidth. The average intensity can be replaced by the mean

$$\bar{I} = MI(\mu, \nu). \quad (5)$$

The averaging over sufficiently thin shells into which the cloud is divided leads to an additional integration of (2) over the radius, which reduces to the simulation of yet another random variable that gives the distance from the cloud center to the common point of the bundle of directions used to compute the mean (5):

$$r = \{r_{in}^3 + R(r_{out}^3 - R_{in}^3)\}^{1/3}, \quad (6)$$

where r_{in} and r_{out} are the radii of the inner and outer boundaries of the shell, and R is a random variable that is uniformly distributed in the interval 0 to 1. The intensity $I(\mu, \nu)$ for a given direction can be estimated by using

$$\begin{aligned} I_\nu(\mu) &= I_{\nu bg}(\mu) \exp \left\{ -\int_0^L x_\nu(y) dy \right\} \\ &+ \int_0^L \varepsilon_\nu(X) \exp \left\{ -\int_0^X x_\nu(y) dy \right\} dX, \end{aligned} \quad (7)$$

where x_ν and ε_ν are the absorption and emission coefficients of the medium, respectively; L is the distance to the cloud edge in the direction of integration; and $I_{\nu bg}$ is the intensity of the background emission for a given direction. The integration path is broken up into segments in which the emission and absorption coefficients can be assumed to be constant (in the presence of a velocity gradient, this path can be much shorter than the path within a single shell where the populations are assumed to be constant). The change in intensity within a segment can be obtained by integrating (7):

$$\Delta I_\nu = \left(\frac{\varepsilon_\nu}{x_\nu} - I_{in} \right) (1 - e^{-x_\nu l}), \quad (8)$$

where I_{in} is the intensity at the beginning of the segment, and l is the segment length in the direction under consideration. The emission and absorption coefficients are expressed in terms of the level populations

$$\varepsilon_\nu = \frac{h\nu}{4\pi} f(\nu) A_{ul} n_u, \quad (9)$$

$$x_\nu = \frac{c^2 A_{ul} f(\nu)}{8\pi\nu^2} \left\{ \frac{g_u}{g_l} n_l - n_u \right\}, \quad (10)$$

where A_{ul} is the Einstein coefficient for the corresponding transition; n_u , g_u and n_l , g_l are the populations and statistical weights of the upper and lower levels, respectively. Thus, the average intensity is expressed in terms of the level populations and the intensity of the background radiation, which allows us to implement the iterative process using the system of statistical-equilibrium equations (1) for the populations. When the iterative process has converged, the derived populations are used to compute the intensity of the cloud radiation (or brightness temperature) with the aid of the formal solution to the transfer equation (7).

RESULTS

We performed the computations for two models with kinetic temperatures of 70 and 20 K and with background-radiation temperatures of 2.7 and 70 K, respectively (below referred to as models I and II respectively). The methanol column densities in the two models were assumed to be the same and equal to $1.5 \times 10^{15} \text{ cm}^{-2}$ (the radius is $1.5 \times 10^{16} \text{ cm}$, the H_2 number density is 10^5 cm^{-3} , and the methanol abundance is 10^{-6}). When computing the models, we took into account 124 lower rotational levels of the ground tor-

sional state of E-methanol ($J < 15$, $|K| < 6$, and $E < 200 \text{ cm}^{-1}$).

Torsional transitions were ignored. We computed the energies of the levels and Einstein coefficients (A) by using approximate formulas from Pikett *et al.* (1981). The collisional constants are known poorly and were computed here in the gas-dynamical approximation of Lees (1974). The iterations were terminated at an accuracy of 0.1% of the population.

DISCUSSION

The algorithm of Bernes (1979) uses the quantity $S_{lu,m'}$ (for the m' shell and for the transition between l and u) which is proportional to the intensity instead of the latter; this quantity is accumulated over all model photons in all shells. A comparison of the system of statistical-equilibrium equations yields the relation $(\sum S_{lu,m'}) = \bar{I}_{lu,m'} B_{lu}$. In each step, according to formula (6) from Bernes (1979), the following quantity is added to $(\sum S_{lu,m'})$:

$$S_{lu,m'} = \frac{h\nu}{4\pi} f(\nu) B_{lu} \frac{s_k W_0 \exp\left(-\sum_{i=1}^{k-1} \tau_i\right)}{V_{m'} \tau_k} \{1 - \exp(-\tau_k)\}, \quad (11)$$

where W_0 is the initial weight of the model photon; $V_{m'}$ is the volume of the m' shell; and τ_i and s_i are the optical depth and path of the model photon in the i th step, respectively. In order to compare the method of Bernes (1979) with the method proposed here, which we deduced from the transfer equation, let us consider the contribution of the intrinsic emission from the m shell, the emission from a different m' shell, and the background radiation to $(\sum S_{lu,m'})$. Substituting the relations for τ_1 and for the initial weight of the model photon produced in the m' shell, $W_0 = V_{m'} A_{ul} n_u / N_{ph}$, where N_{ph} is the total number of model photons, we obtain the following expression for the contribution of the intrinsic emission from the m' shell:

$$S_{lu,m'} = \frac{B_{lu}}{N_{ph}} \left(\frac{2h\nu^3}{c^2} \frac{1}{\frac{n_l g_u}{n_u g_l} - 1} \right) \{1 - \exp(-\tau_1)\}. \quad (12)$$

Since the term in parentheses is the source function and comparing this equation with (8), we conclude that the contribution of the intrinsic emission is accurately represented in the method of Bernes (1979). It follows from (7) that the contribution of the background radiation must be given by

$$S_{lu,m'} = \frac{B_{lu}}{N_{ph}} I_{bg} \exp\left(-\sum_{i=1}^{k-1} \tau_i\right), \quad (13)$$

where I_{bg} is the intensity of the background radiation at the frequency of the transition between levels u and l . If the cloud is divided into shells of equal volume ($V_{m'} = \text{const}$), then the path of the model photon is the same in each step ($s_k = \text{const}$) and small enough for the optical depth in each step to be small in absolute value. Formula (13) can then be derived from (11) by using the linear approximation for the exponent. The contribution of the emission from a different shell can be obtained from (11), by analogy with (12),

$$S_{lu,m'} = \frac{B_{lu}}{N_{ph}} \frac{V_m}{V_{m'}} \exp\left(-\sum_{i=1}^{k-1} \tau_i\right) \times \left(\frac{2h\nu^3}{c^2} \frac{1}{\frac{n_l g_u}{n_u g_l} - 1} \right)_k \{1 - \exp(-\tau_k)\}, \quad (14)$$

where the subscript k of the source function means that this function is calculated from the populations in the k th step (in the m' shell rather than the m shell where the model photon was formed). It follows from (7) that this contribution must be equal to the product of (12), where the source function is calculated from the populations in the first step and the exponential factor from (13). If the cloud is divided into shells of equal volume and if the optical depth in each step is small in absolute value (which allows a linear expansion of the exponent), then, using relation (9) for the emission coefficient, we obtain the last condition for the applicability of the algorithm of Bernes (1979):

$$f_k(\nu)(n_u)_k s_k \approx f_1(\nu)(n_u)_1 s_1, \quad (15)$$

where the subscripts denote the first and k th steps in the propagation of the model photon. Relation (15) is the condition for the equality of the specific column densities of the emitting molecule in each step in the direction of propagation of the model photon. The latter condition is most stringent and is difficult to satisfy in practice. Since uncertainty in the estimate of the radiation field in the algorithm of Bernes (1979) produces additional noise in the method, the use of the algorithm outlined here seems more appropriate. Our method correctly describes the radiation field (the formulas follow from the transfer equation); therefore, its application is restricted only by the convergence of the iterative procedure used (matches the iterative procedure in the classical MC method) and by the available computing time. In practice, the convergence can be hampered in the presence of strong masers.

The qualitative behavior of populations in the limiting cases of hot gas (model I) and hot background radiation (model II) is convenient to analyze as follows. Let us consider the relation between the ratio of the level population to its statistical weight and the energy of this level on a logarithmic scale. In order not to overload the picture, let us consider only the ladders with quan-

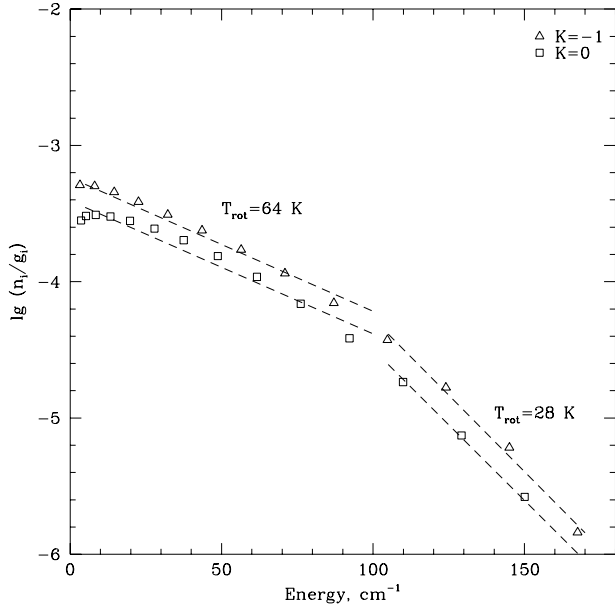


Fig. 1. Logarithm of the ratio of the population (in cm^{-3}) to the statistical weight versus the energy of a given level for the model with a background-radiation temperature of 2.7 K and a cloud kinetic temperature of 70 K. The dashed lines correspond to rotational temperatures of 64 and 28 K.

tum numbers $K = 0$ and -1 . In the LTE case, the level population would be given by Boltzmann formula, and we would have a straight line whose slope would be related to the temperature. In the non-LTE case, however, we have a curve (Figs. 1 and 2). The levels that correspond to the different ladders in these figures are indicated by different symbols. In the model with hot gas, the $K = -1$ ladder is heavily overpopulated relative to the $K = 0$ ladder at small quantum numbers J , while in the radiation-dominated model, the $K = 0$ ladder lies above the $K = -1$ ladder; i.e., there is an inversion of other transitions. This may correspond to the division of methanol masers into class I (Fig. 1) and class II (Fig. 2) masers (Batra *et al.* 1987; Menten *et al.* 1991). The slope of the curve at energies $E < 100 \text{ cm}^{-1}$ in Fig. 1 corresponds to a rotational temperature $T_{\text{rot}} \sim 64 \text{ K}$, which is close to the kinetic temperature of the medium. At high energies, $T_{\text{rot}} \sim 28 \text{ K}$. In Fig. 2, rotational temperatures $T_{\text{rot}} \sim 27 \text{ K}$ (which is close to the kinetic temperature of the medium) and $T_{\text{rot}} \sim 59 \text{ K}$ (which is close to the background-radiation temperature $T_{\text{bg}} = 70 \text{ K}$) correspond to low and high energies, respectively. Thus, the slope of the curve appears to be mainly determined by collisions at low energies and by radiation at high energies. The distribution of populations within the ladder (in each of the segments) is close to the Boltzmann distribution, while, between the ladders, it is a purely non-LTE distribution. For this reason, no emission arises in a-type transitions ($\Delta K = 0$).

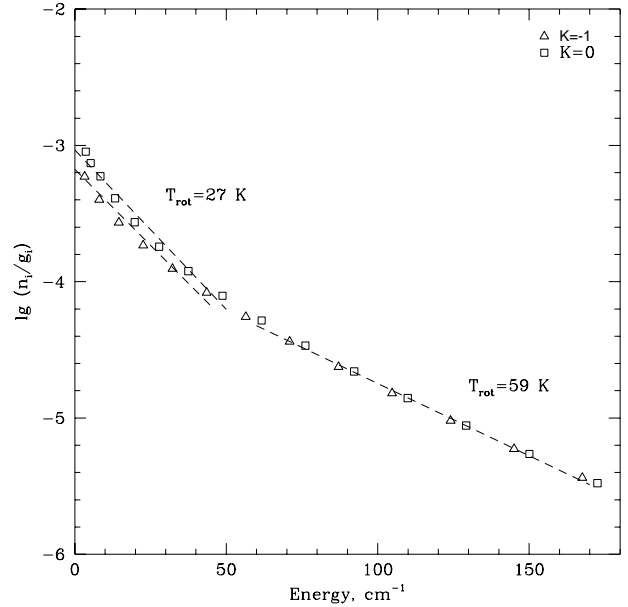


Fig. 2. Same as Fig. 1 for the model with a background-radiation temperature of 70 K and a cloud kinetic temperature of 20 K. The dashed lines correspond to rotational temperatures of 27 and 59 K.

The b-type transitions (which occur with a change in the quantum number K) tend to produce a series of the form $(J+\alpha)_{K\pm 1} - J_K$, where $\alpha = 0, \pm 1$ (Menten *et al.* 1986b). Since the series $J_0 - (J+1)_{-1}$ includes transitions from the $K=0$ ladder to the $K=-1$ ladder and vice versa, some of the transitions in this series exhibit activity in model I ($4_{-1} - 3_0, 5_{-1} - 4_0$, etc.), and other are active in model II ($0_0 - 1_{-1}, 1_0 - 2_{-1}, 2_0 - 3_{-1}$). Masers in this series were detected in the observations of Turner *et al.* (1972), Zuckerman *et al.* (1972), Batra *et al.* (1987), and Slysh *et al.* (1997, 1999). In the models under consideration, the series $J_0 - J_{-1}$ at 157 GHz gives a weak inversion of transitions for $J=2$ and 3. Masers in this series were detected in the observations for $2 \leq J \leq 8$ (Slysh *et al.* 1995). The transitions in the series $J_0 - (J-1)_{-1}$ have higher frequencies and show no inversion in the models under consideration. A similar behavior of the populations is observed for transitions between other ladders. The $(J+1)_0 - J_1$ transitions exhibit class I and II activity for $J > 2$ and $J < 3$, respectively. Wilson *et al.* (1985) detected a maser in the $2_1 - 3_0$ line at 20 GHz. Slysh *et al.* (1992) identified weak thermal emission in the $4_0 - 3_1$ line at 28 GHz. The series $J_1 - J_0$ at 165 GHz and $J_1 - (J-1)_0$ give no inversion in the models under discussion. No masers in the series $J_1 - J_0$ were detected in the observations of Slysh *et al.* (1999). The transitions in the series $J_2 - J_1$ at 25 GHz give an inversion in model I. No masers in this series were detected in the observations of Barret *et al.* (1971) and

Peak optical depths of the lines for models with the following H_2 number densities, methanol abundances, kinetic temperatures, and background-radiation temperatures: 1 - $n_{H_2} = 10^5 \text{ cm}^{-3}$, $X = 10^6$, $T_{kin} = 70 \text{ K}$, and $T_{bg} = 2.7 \text{ K}$; 2 - $n_{H_2} = 10^5 \text{ cm}^{-3}$, $X = 10^6$, $T_{kin} = 20 \text{ K}$, and $T_{bg} = 70 \text{ K}$

Transition	Frequency, GHz	1 τ		2 τ	Transition	Frequency, GHz	1 τ		2 τ
$0_0 - 1_{-1}$	108.9	2.0	M2 ^a	-2.0*	$4_0 - 3_1$	28.3	-0.7*	-M ^g	3.0
$1_0 - 0_0$	48.4	-0.2*		2.4	$4_0 - 3_0$	193.4	0.7		7.8
$1_0 - 1_{-1}$	157.3	2.6		1.6	$4_0 - 4_{-1}$	157.2	9.8	M2 ^b	0.1
$1_0 - 2_{-1}$	60.5	3.8		-4.3*	$4_1 - 3_2$	168.6	0.7		-0.2*
$1_1 - 0_0$	213.4	0.4		3.0	$4_1 - 3_1$	193.5	0.8		7.4
$1_1 - 1_0$	165.1	1.0	-M ^a	0.4	$4_1 - 4_0$	165.2	3.2	-M ^a	1.2
$1_1 - 2_0$	68.3	0.4		-1.1*	$4_2 - 3_2$	193.5	1.0		2.5
$2_{-2} - 3_{-1}$	278.3	1.2		0.1	$4_2 - 3_1$	218.4	-1.2*		13.9
$2_{-1} - 1_{-1}$	96.7	-1.0*		4.7	$4_2 - 4_1$	24.9	-2.3*	M1 ^e	5.3
$2_0 - 1_0$	96.7	-0.1*		4.4	$4_3 - 3_3$	193.5	0.1		1.0
$2_0 - 1_{-1}$	254.0	0.8		1.9	$4_3 - 5_2$	288.7	0.9		0.1
$2_0 - 2_{-1}$	157.3	6.2	M2 ^b	-0.3*	$5_{-4} - 4_{-4}$	241.8	0.0		0.6
$2_0 - 3_{-1}$	12.2	4.9	M2 ^c	-6.7*	$5_{-4} - 6_{-3}$	234.7	0.0		0.0*
$2_1 - 1_1$	96.8	-0.2*		3.5	$5_{-3} - 4_{-3}$	241.9	0.2		1.7
$2_1 - 1_0$	261.8	0.8		4.4	$5_{-2} - 4_{-2}$	241.9	1.3		3.9
$2_1 - 2_0$	165.1	1.6	-M ^a	1.0	$5_{-2} - 6_{-1}$	133.6	2.8	-M ^h	-0.6*
$2_1 - 3_0$	20.0	0.6	M2 ^d	-2.6*	$5_{-1} - 4_0$	84.5	-3.7*	M1 ⁱ	4.4
$2_2 - 1_1$	121.7	-2.2*		22.2	$5_{-1} - 4_{-1}$	241.8	3.1		6.3
$2_2 - 2_1$	24.9	-1.0*	M1 ^e	7.6	$5_0 - 4_1$	76.5	-0.7*		2.6
$3_{-2} - 2_{-2}$	145.1	-0.3*		2.6	$5_0 - 4_0$	241.7	1.5		6.9
$3_{-2} - 4_{-1}$	230.0	2.1	-M ^a	-0.1*	$5_0 - 5_{-1}$	157.2	9.6	M2 ^b	0.6
$3_{-1} - 2_{-1}$	145.1	0.1		6.9	$5_1 - 4_2$	216.9	1.1		0.4
$3_0 - 2_0$	145.1	0.2		7.7	$5_1 - 4_1$	241.9	1.4		6.4
$3_0 - 3_{-1}$	157.3	8.7	M2 ^b	-0.5*	$5_1 - 5_0$	165.4	3.9	-M ^a	1.2
$3_1 - 2_2$	120.2	0.2		-0.5*	$5_2 - 4_2$	241.9	1.7		3.1
$3_1 - 2_1$	145.1	0.2		6.5	$5_2 - 4_1$	266.8	-0.3*		9.3
$3_1 - 3_0$	165.1	2.3	-M ^a	0.9	$5_2 - 5_1$	25.0	-2.2*	M1 ^e	3.0
$3_2 - 2_2$	145.1	0.0*		1.6	$5_3 - 4_3$	241.8	0.4		1.6
$3_2 - 2_1$	170.1	-2.0*		19.0	$5_3 - 6_2$	240.2	1.2		0.1
$3_2 - 3_1$	24.9	-2.0*	M1 ^e	7.9	$5_4 - 4_4$	241.8	0.0		0.5
$4_{-4} - 5_{-3}$	283.1	0.0		0.0	$6_{-5} - 5_{-5}$	290.1	0.0		0.3
$4_{-3} - 3_{-3}$	193.5	0.0		1.2	$6_{-4} - 5_{-4}$	290.2	0.1		1.0
$4_{-2} - 3_{-2}$	193.5	0.5		3.5	$6_{-4} - 7_{-3}$	186.3	0.0		0.0*
$4_{-2} - 5_{-1}$	181.8	2.7		-0.4*	$6_{-3} - 5_{-3}$	290.2	0.3		1.8
$4_{-1} - 3_0$	36.2	-4.5*	M1 ^f	5.5	$6_{-2} - 5_{-2}$	290.3	1.9		3.7
$4_{-1} - 3_{-1}$	193.4	1.6		6.8	$6_{-2} - 7_{-1}$	85.6	2.8		-0.6*

Table. (Contd.)

Transition	Frequency, GHz	1 τ		2 τ	Transition	Frequency, GHz	1 τ		2 τ
$6_{-1} - 5_0$	132.9	-2.7*	M1 ^g	3.4	$8_2 - 8_1$	25.3	-1.3*	M1 ^e	0.3
$6_{-1} - 5_{-1}$	290.1	4.2		5.5	$8_3 - 9_2$	94.5	0.8		-0.1*
$6_0 - 5_1$	124.6	-0.6*		2.2	$9_{-5} - 10_{-4}$	268.7	0.0		0.0
$6_0 - 5_0$	289.9	2.4		5.7	$9_{-4} - 10_{-3}$	41.1	0.0*		-0.1*
$6_0 - 6_{-1}$	157.0	8.8	M2 ^b	0.7	$9_{-3} - 10_{-2}$	282.0	0.4		0.0
$6_1 - 5_2$	265.3	1.4		0.9	$9_{-1} - 8_0$	278.3	-0.5*		1.5
$6_1 - 5_1$	290.3	1.9		5.2	$9_{-1} - 8_{-2}$	9.9	-2.0*	M1 ^k	0.5
$6_1 - 6_0$	165.7	4.0		1.0	$9_0 - 8_1$	267.4	0.1		1.1
$6_2 - 5_2$	290.3	2.3		3.3	$9_0 - 9_{-1}$	156.0	5.1		0.5
$6_2 - 6_1$	25.0	-1.9*	M1 ^e	1.5	$9_1 - 9_0$	167.9	2.4		0.5
$6_3 - 5_3$	290.2	0.7		1.9	$9_2 - 9_1$	25.5	-1.0*	M1 ^l	0.1
$6_3 - 7_2$	191.7	1.2		0.0*	$9_3 - 10_2$	45.8	0.6		-0.1*
$6_4 - 5_4$	290.2	0.1		0.8	$10_{-5} - 11_{-4}$	220.4	0.0		0.0
$6_5 - 5_5$	290.1	0.0		0.2	$10_{-3} - 11_{-2}$	232.9	0.2		0.0
$7_{-4} - 8_{-3}$	137.9	0.0		-0.1*	$10_{-1} - 9_{-2}$	57.3	-1.4*		0.4
$7_{-2} - 8_{-1}$	37.7	2.4	M2 ^j	-0.6*	$10_0 - 10_{-1}$	155.3	3.7		0.4
$7_{-1} - 6_0$	181.3	-1.8*		2.6	$10_1 - 10_0$	169.3	1.6		0.3
$7_0 - 6_1$	172.4	-0.3*		1.8	$10_2 - 10_1$	25.9	-0.7*		0.0
$7_0 - 7_{-1}$	156.8	7.7	M2 ^b	0.7	$11_{-5} - 12_{-4}$	172.1	0.0		0.0*
$7_1 - 7_0$	166.2	3.7		0.8	$11_{-3} - 10_{-4}$	7.3	0.0		0.1
$7_2 - 7_1$	25.1	-1.6*	M1 ^e	0.7	$11_{-3} - 12_{-2}$	183.7	0.1		0.0
$7_3 - 8_2$	143.2	1.1		-0.1*	$11_{-1} - 10_{-2}$	104.3	-0.9*		0.3
$8_{-4} - 9_{-3}$	89.5	0.0		-0.1*	$11_0 - 11_{-1}$	154.4	2.4		0.3
$8_{-1} - 7_0$	229.8	-1.0*	M1 ^a	2.0	$11_1 - 11_0$	171.2	0.8		0.3
$8_0 - 7_1$	220.1	-0.1*		1.4	$11_2 - 10_3$	2.9	-0.3*		0.1
$8_0 - 8_{-1}$	156.5	6.5	M2 ^b	0.6	$11_2 - 11_1$	26.3	-0.4*		0.0*
$8_1 - 8_0$	166.9	3.2		0.6	$11_4 - 12_3$	253.9	0.0		0.0

Note: M1 – a class I maser was observed; M2 – a class II maser was observed; –M – no maser was detected; * – the optical depth in this transition is negative; (a) – Slysh *et al.* (1999); (b) – Slysh *et al.* (1995); (c) – Batrla *et al.* (1987); (d) – Wilson *et al.* (1985); (e) – Barret *et al.* (1971); (f) – Turner *et al.* (1972); (g) – Slysh *et al.* (1992); (h) – Slysh *et al.* (1997); (i) – Zuckerman *et al.* (1972); (j) – Haschick *et al.* (1989); (k) – Slysh *et al.* (1993); (l) – Menten *et al.* (1986a).

Menten *et al.* (1986a). Inversion in class I models is also observed for the transitions of the series $(J+1)_2 - J_1$. The first two transitions in the series ($J = 1$ and 2) turn out to show the greatest inversion. In model II, inversion is observed in the $3_1 - 2_2$ transition from the series $(J+1)_1 - J_2$. Since the series $J_{-2} - (J+1)_{-1}$ contains transitions from $K = -2$ ladder to the $K = -1$ ladder and vice versa, some of the transitions show inversion in model I ($9_{-1} - 8_{-2}$, $10_{-1} - 9_{-2}$, etc.), and others show inversion in model II ($5_{-2} - 6_{-1}$, $6_{-2} - 7_{-1}$, $7_{-2} - 8_{-1}$; transitions with smaller J have higher frequencies and show no inversion or their inversion is marginal). The lowest frequency transitions $7_{-2} - 8_{-1}$ at 37 GHz and $9_{-1} - 8_{-2}$ at 9.9 GHz, which were observed in the direction of star-forming regions (Haschick *et al.* 1989; Slysh *et al.* 1993), are the most intense transitions in this series. No

maser emission was detected in the $5_{-2} - 6_{-1}$ and $3_{-2} - 4_{-1}$ transitions (Slysh *et al.* 1999). The series $(J+1)_2 - J_3$ ($J > 9$) gives inversion in model I. The optical depth in transitions between ladders with different K is small because of the low population (although inversion may exist). Our computations are in qualitative agreement with the data of Cragg *et al.* (1992), which were obtained by the LVG method. Candidates for class II masers coincide with those of Sobolev *et al.* (1997), with the exception of the series $J_1 - J_0$ at 165 GHz. This result may be related to the difference in the model parameters. Peak optical depth for the lines with frequencies below 300 GHz up to $J = 11$ inclusive in models I and II are given in the table. When computing the spectra, we assumed that all sources were observed

against the background radiation with a temperature of 2.7 K.

CONCLUSION

(1) The method of Bernes (1979) is applicable if the cloud is divided into shells of equal volume, if the paths of model photons and the optical depths in each step are sufficiently small, and if the column densities of the emitting molecule in the direction of propagation of the model photon are equal for each step. The applicability of the method proposed here is restricted only by the convergence of the iterative procedure, which may be hampered in the presence of strong masers.

(2) The populations within the ladder (Figs. 1 and 2) in the segments before and after the break are well described by the Boltzmann formula, while the populations between the ladders have a non-LTE distribution. For this reason, no masers are formed in transitions that occur with no change in the quantum number K . The position of the break in the "logarithm of population-to-statistical-weight ratio versus level energy" diagram appears to be determined by the ratio of the rates of collisions and radiative processes.

(3) The transitions $2_2 - 1_1$ at 121 GHz, $3_2 - 2_1$ at 170 GHz, $10_2 - 10_1$ and $11_2 - 11_1$ at 26 GHz, $5_0 - 4_1$ at 76 GHz, $6_0 - 5_1$ at 124 GHz, $7_0 - 6_1$ at 172 GHz, $7_{-1} - 6_0$ at 181 GHz, $10_{-1} - 9_{-2}$ at 57 GHz, $11_{-1} - 10_{-2}$ at 104.3 GHz, $11_2 - 10_3$ at 2.9 GHz are candidates for new class I masers, while the transitions $1_0 - 2_{-1}$ at 61 GHz, $1_1 - 2_0$ at 68 GHz, and $6_{-2} - 7_{-1}$ at 86 GHz are candidates for class II masers.

ACKNOWLEDGEMENTS

I wish to thank V.I. Slysh for several valuable remarks and helpful discussions which undoubtedly improved the content of this paper, A.M. Dzura for valuable recommendations and remarks on the implementation of Bernes' algorithm, and S.V. Kalenskii for valuable remarks on the pumping mechanism. I also wish to thank A.M. Sobolev and A.A. Kalinin for a discussion of the method. This study was supported in part by the Russian Foundation for Basic Research (project nos. 97-02-27241 and 96-02-00848) and the Radio

Astronomy Research and Education Center (project no. 315).

REFERENCES

- Barrett, A.H., Schwartz, P.R., and Waters, J.W., *Astrophys. J.*, 1971, vol. 168, p. L101.
 Batrla, W., Mattheus, H.E., Menten, K.M., and Walmsley C.M., *Nature*, 1987, vol. 326, p. 49.
 Bernes, C., *Astron. Astrophys.*, 1979, vol. 73, p. 67.
 Cragg, D.M., Johns, K.P., Godfrey, P.D., Brown, R.D., *Mon. Not. R. Astron. Soc.*, 1992, vol. 259, p. 203.
 Haschick, A.D., Baan, W.A., and Menten, K.M., *Astrophys. J.*, 1989, vol. 346, p. 330.
 Juvela, M., *Astron. Astrophys.*, 1997, vol. 322, p. 943.
 Lees, H., *Can. J. Phys.*, 1974, vol. 52, p. 2250.
 Menten, K.M., *Proc. Third Haystack Observatory Meeting*, Haschick, A.D. and Ho, P.T.P., Eds., 1991, p. 119.
 Menten, K.M., Reid, M.J., Moran, J.M., Wilson, T.L., Johnston, K.J., and Batrla, W., *Astrophys. J.*, 1988, vol. 333, p. L83.
 Menten, K.M., Walmsley, C.M., Henkel, C., and Wilson, T.L., *Astron. Astrophys.*, 1986a, vol. 157, p. 318.
 Menten, K.M., Walmsley, C.M., and Henkel, C., *Astron. Astrophys.*, 1986b, vol. 169, p. 271.
 Pickett, H.M., Cohen, E.A., Brinza, D.E., and Shafer, M.M., *J. Mol. Spectrosc.*, 1981, vol. 89, p. 542.
 Slysh, V.I., Kalenskii, S.V., and Val'tts, I.E., *Astron. Astrophys.*, 1993, vol. 413, p. L133.
 Slysh, V.I., Kalenskii, S.V., and Val'tts, I.E., *Astrophys. J.*, 1992, vol. 397, p. L43.
 Slysh, V.I., Kalenskii, S.V., and Val'tts, I.E., *Astrophys. J.*, 1995, vol. 442, p. 668.
 Slysh, V.I., Kalenskii, S.V., Val'tts, I.E., and Golubev, V.V., *Astrophys. J.*, 1997, vol. 478, p. L37, astro-ph/9701075
 Slysh, V.I., Val'tts, I.E., and Kalenskii, S.V., *Astron. Astrophys.*, 1999 (in press)
 Sobolev, A.M., Cragg, D.M., and Godfrey, P.D., *Mon. Not. R. Astron. Soc.*, 1997, vol. 288, p. L39.
 Turner, B.E., Gordon, M.A., and Wrixon, G.T., *Astrophys. J.*, 1972, vol. 177, p. 609.
 Wilson, T.L., Walmsley, C.M., Menten, K.M., and Hermsen, W., *Astron. Astrophys.*, 1985, vol. 147, p. L19.
 Zuckerman, B., Turner, B.E., Johnson, D.R., Palmer, P., and Morris, M., *Astrophys. J.*, 1972, vol. 177, p. 609.

Translated by V. Astakhov